ISBN: 978-3-95450-132-8 doi:10.18429/JACoW-IPAC2014-THPRO078

TIME-DEPENDENT BEHAVIOUR OF GAS EJECTED FROM AN ACCELERATING STRUCTURE AFTER A DISCHARGE

V. Ziemann, Uppsala University, Uppsala, Sweden

Abstract

A discharge or RF-breakdown event in a CLIC acceleration structure causes the localized release of gas molecules inside a thin conduction limited system with distributed pumping. We discuss the transient behavior of such a system in the molecular flow regime that allows an analytical solution with the help of Greens functions. They describe the temporal evolution of the gas density and the gas flow ejected from the ends of thin pipes of finite length. Distributed pumping, for example through the HOM damping slits is taken into account.

INTRODUCTION AND MODEL

We calculate the temporal evolution of the gas density following a spontaneous injection of a known amount of gas in a thin pipe with or without distributed pumping. Examples of such systems are radio-frequency structures for linear accelerators that experience a discharge due to high power levels. Below we show that the pressure distribution inside the pipe as well as the amount of gas ejected from the end of the pipe as a function of time can be calculated analytically. This allows to estimate the behavior of such a system without computer simulations and might be useful in debugging numerical codes or calibrating hardware such as pumps. We assume that only a reasonably small amount of gas is desorbed at each particular event such that we can assume to operate in the molecular flow regime under isothermal conditions. In this case there is no interaction among gas molecules and that the interactions with the walls of the vacuum vessel can be described by diffuse scattering. Under these conditions the time dependent pressure profile $P(z,t)$ along a conduction limited pipe of length l with $0 < z < l$ obeys the following partial differential equation [1]

$$v\frac{\partial}{\partial t}P = \frac{\partial}{\partial z}c\frac{\partial}{\partial z}P - sP + q \qquad (1)$$

with the volume $V = vl$ of the pipe and the conductance $C = c/l$, the pump speed $S = sl$ and the out-gassing rate $Q = ql$. In these equations the 'per-length' quantities q, v, s are implicitly defined. For practical purposes it is worth noting that for a round pipe with radius r the conductance C depends on the mass of a gas molecule m and the absolute temperature T through the Knudsen equation [2]

$$C = \frac{4}{3}\sqrt{\frac{2\pi kT}{m}}\frac{r^3}{l} \qquad (2)$$

where k is the Boltzmann constant. For a general cross section the conductance can be calculated by the Smoluchowski formula, eq. 4.152 in [3].

The specific conductance c is constant for given mass and temperature in the pipe and we can therefore rewrite Eq. 1 as

$$\frac{\partial P}{\partial t} = D\frac{\partial^2 P}{\partial z^2} - \frac{1}{\tau}P \qquad (3)$$

with the diffusion constant $D = c/v$ and the pump-down time scale $1/\tau = s/v$. Note that the physical parameters such as particle species and temperature that determine the gas dynamics are contained in the two parameters D and τ.

We briefly comment on the limits of applicability of the diffusion equation which is mainly determined by the diffusion constant D and the pump speed s, both assumed to be constant which is not entirely justified. First, eq. 2 is strictly valid only for long pipes. For shorter pipes eq. 4.158 in [3] indicates that the conductance varies by up to 13 % from eq. 2 leading normally to an overestimate of the diffusion constant D in the range of a several times the pipe diameter from the gas source. Second, the pump speed s, is affected by the fact that the flow far away from the gas source becomes more directional. This is the so-called beaming effect. The transverse flow pattern at the end of a long pipe is, for example, shown in [4] and indicates that the transverse flow-profile as a function of radius ρ is given by the elliptic integral [5] $E(\rho/r)$ which is unity at the surface of the pipe at $\rho = r$ and $\pi/2$ in the center at $\rho = 0$. Averaging this over the entire aperture yields 4/3 and eventually leads to eq. 2. Thus the flow or the number of molecules near the surface, where the pumps are located is reduced to 75 % compared to the average flow. Since we use eq. 2 in eq. 3 we conclude that far away from the gas source we underestimate the pump speed by about 25 % at distances sufficiently far away from the gas source where significant beaming has developed.

Returning to the problem at hand, eq. 3 can be solved [6] by means of Fourier transforming the spatial coordinate z of the pressure $P(z,t)$

$$P(z,t) = \frac{1}{2\pi}\int_{-\infty}^{\infty}\tilde{P}(k,t)e^{-ikz}dk\,. \qquad (4)$$

After inserting in Eq. 3 and separating variables we obtain $d\tilde{P}/\tilde{P} = -(k^2D+1/\tau)dt$ which can be trivially integrated to yield $\tilde{P}(k,t) = P_0\, e^{-(k^2D+1/\tau)t}$, where P_0 is the integration constant that corresponds to the initial pressure at time $t = 0$. Performing the inverse Fourier transform to leads to the pressure as a function of the spatial variable z

$$P(z,t) = \frac{\tilde{P}_0}{\sqrt{4\pi Dt}}\, e^{-t/\tau}e^{-z^2/4Dt} \qquad (5)$$

which we recognize as a spreading Gaussian with rms width $\sqrt{2Dt}$ – the well-known solution of the diffusion equa-

ISBN: 978-3-95450-132-8 doi:10.18429/JACoW-IPAC2014-THPRO078

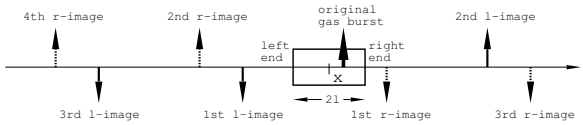

Figure 1: The location of the image gas loads.

tion [7] – that is decaying exponentially with the pump-down time scale τ. Instead of using the pressure we now introduce the longitudinal density of molecules dN/dz which is related to the pressure P by $P = kTdN/dzv$. This allows us to rewrite Eq. 5 as

$$\frac{dN}{dz}(z,t) = \frac{N_0}{\sqrt{4\pi Dt}} \exp\left[-\frac{(z-z_0)^2}{4Dt}\right] e^{-t/\tau} \qquad (6)$$

which is intuitively appealing. Here N_0 is the number if initially released gas molecules. Equation 6 fulfills the differential equation in Eq. 3 but does not obey the boundary conditions at the ends of the pipe where we assume that the pipe is connected to a large reservoir with big pumps. The proper boundary condition at the ends is therefore $dN/dz|_{end} \approx 0$ and we will now make sure that the solution fulfills this requirement.

SOLUTION

We can construct a solution that satisfies the boundary condition by introducing the concept of 'image gas loads' inspired by [8] and imagine that the pipe extends infinitely to both sides and place a virtual gas source that causes a negative particle distribution which also obeys the differential equation Eq. 1. If the distance from the real gas source to the pipe end equals that of the virtual source, the sum of both distributions will add up to zero at all times t. In Fig. 1 the first right image gas load is labeled '1st r-image' and since it is negative, the arrow points down.

Of course the first image gas load also has a non-zero contribution on the left pipe end which in turn requires a further image load (2nd r-image) far to the left that compensates this, but in turn causes a small error at the other end on the right side which requires a further compensation (3rd r-image). The same is true for the image gas load (1st l-image) that initially forces the pressure to zero on the left end and generates a small error on the right end which requires the image gas load labeled 2nd l-image to correct. We therefore find that we have two cascades of image gas loads shown in Fig. 1, one with dotted arrows for the right end and one with solid arrows for the left end.

The positions of the first few image gas loads are easily calculated by hand. We start with the r-images. If the initial burst occurs a distance x to the right of the center of the pipe that has a length $2l$, the first r-image is located at $x_1 = l + (l - x) = 2l - x$. The 2nd r-image is located when we mirror x_1 at the left exit and find the location $x_2 = -l - (l + x_1) = -2l - x_1 = -4l + x$. Continuing in the same way, by mirroring x_2 at the right exit we find the location of the third

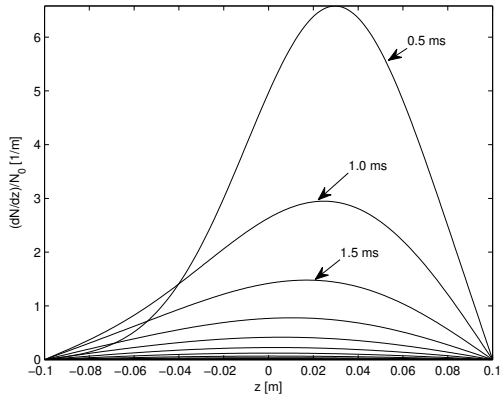

Figure 2: The evolution of the particle density distribution after the initial gas burst at $z = 0.03$ m from 0.5 ms to 10 ms in steps of 0.5 ms. The curves for 0.5, 1.0, and 1.5 ms are indicated in the figure. The curves at subsequent times get continuously smaller but are not individually labeled.

image gas load to be $x_3 = l + (l - x_2) = 2l - (-4l + x) = 6l - x$. This scheme can be continued and we find that the locations of the r-images are given by $x_n = (-1)^{n-1}(2nl - x)$ because there is a term $2l$ picked up at every mirroring process. The same procedure can be applied to determine the locations of the images to accommodate the boundary conditions at the left exit and we find $y_n = (-1)^n(2nl + x)$. Note that the locations of the image gas loads x_n and y_n rapidly increase by $2l$ in every iteration and since each image gas load is described by a spreading Gaussian, we can expect rapid convergence.

At each of the locations x_n and y_n we now place an image gas load with the appropriate sign. The dynamics of each such load is given by Eq. 6 and the distribution that fulfills the boundary condition to have zero pressure at the exit is given by

$$\frac{dN}{dz}(z,t) = \frac{N_0 e^{-t/\tau}}{\sqrt{4\pi Dt}} \left\{ e^{-(z-x)^2/4Dt} + \sum_{n=1}^{\infty} (-1)^n \left[e^{-(z-x_n)^2/4Dt} + e^{-(z-y_n)^2/4Dt} \right] \right\} \qquad (7)$$

where the first term in the curly braces describes the distribution of the initial gas burst. The sum has two exponential terms which describe the image gas load distributions at locations x_n and y_n that suitably alternate sign. Since the locations x_n and y_n appear quadratically in the argument of the exponentials we can expect rapid convergence. It is easy to implement Eq. 7 in Matlab and add terms in the sums until they are below a threshold. We found that normally less than 10 terms in the sum are sufficient. dN/dz in eq. 7 describes the number of particles in a small interval dz along the pipe after a time t if N_0 gas molecules are injected at position x and thus constitutes the sought Greens function.

ISBN: 978-3-95450-132-8 doi:10.18429/JACoW-IPAC2014-THPRO078

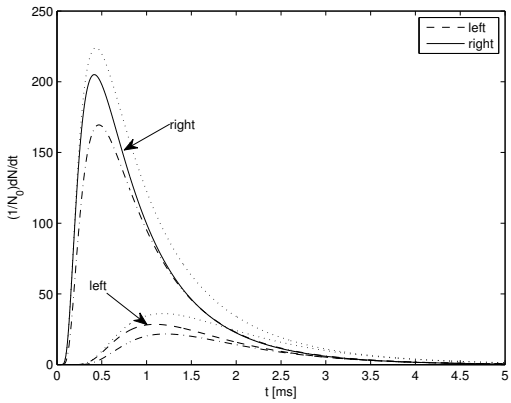

Figure 3: The number of molecules ejected from the ends of the thin pipe as a function of time. The solid and the dashed line indicate the profiles at the right and left ends for nominal conditions. The dotted lines indicate the profiles where the pump strength is reduced by 25 % and the dot-dashed lines where the diffusion constant is reduced by 13 %, respectively from their nominal values.

Apart from the particle distribution inside the pipe that rate at which particles are ejected from the ends of the pipe is important, because it carries the information about the location of the initial gas burst. We therefore calculate the gas flow $Q = -cdP/dz$ or, equivalently, the rate of ejected particles $dN/dt = Q/kT$. Using Eq. 7 and performing the derivative with respect to z we find

$$\frac{dN}{dt} = -\frac{DN_0}{4\sqrt{\pi}}\frac{1}{(Dt)^{3/2}}\left\{F(z,x) + \sum_{i=1}^{\infty}(-1)^n\left[F(z,x_n)+F(z,y_n)\right]\right\} \quad (8)$$

for $z = \pm l$ and $F(z,x) = (z-x)e^{-(z-x)^2/4Dt}$. The equations for the particle distribution Eq. 7 and the ejected particle rate Eq. 8 constitute the main results of this paper.

EXAMPLE

To illustrate this result we assume that we are dealing with nitrogen gas at room temperature and we consider a 20 cm long thin pipe with a radius of 5 mm. This leads to a value of the diffusion constant $D = 1.65\,\mathrm{m}^2/\mathrm{s}$. Furthermore we assume distributed pumping with a pump strength of $s = 6.4 \times 10^{-2}\,\mathrm{m}^2/\mathrm{s}$ which could come from four radial pumping slits with a length of 50 mm and a radius of 2 mm spaced every 10 mm. Each of the slits has a conductance of $1.6 \times 10^{-4}\,\mathrm{m}^3/\mathrm{s}$ and will limit the pumping capacity of any sizeable pump at the remote end of the slits. For the pump-down time scale we find $\tau = 1.2$ ms.

In Fig. 2 we show the evolution of the longitudinal particle density dN/dz from 0.5 ms to 10 ms in steps of 0.5 ms when the initial burst occurs a little to the right of the center at $z = 0.03$ m. We clearly see that the distribution is asymmetric and that the boundary conditions $dN/dz = 0$ at $z = \pm l = \pm 0.1$ m are fulfilled. In Fig. 3 we show the number of ejected particles for the same system. The number ejected from the exit closer to the initial burst (solid) shows a much stronger and slightly quicker signal compared to the ejected rate from the remote exit (dashed) as can be intuitively expected.

In order to estimate the experimental predictability of the method we repeated the analysis with the rather pessimistic assumption that the pump speed s is reduced by 25 % to account for beaming as discussed above and plot the corresponding profiles as dotted lines in Fig. 3. The peaks of the gas ejection rate are enhanced by about 10 % but the shape is essentially unaffected. Then we repeated the calculation with the equally pessimistic assumption that the diffusion constant is reduced by 13 % and show the profiles as dot-dashed lines in Fig. 3. We find that the profiles are less peaked by approximately 15 % but, again, have essentially the same shape as the unperturbed profiles. We also note that the effect of reduced pump speed and reduced diffusion have opposite effect and cancel to a large extent.

CONCLUSIONS

We derived a solution a for the time dependent pressure profile and gas ejection rate from a pipe that is exposed to a localized injection of a finite amount of gas. The analysis is based on a diffusion model of the gas dynamics and we estimated the limits of validity of the method to be on the 10 to 15 % level, mostly due to effect of beaming and variation of the conductance, and thereby the diffusion constant, as a function of the distance from the gas source.

This work is supported by the 7th European Framework program EuCARD under grant number 227579.

REFERENCES

[1] V. Ziemann, Vacuum 81 (2007) 866-870.

[2] M. Knudsen, Annalen der Physik 28 (1909) 75.

[3] K. Jousten (Ed), Handbook of Vacuum Technology, Wiley-VCH, Weinheim, 2008.

[4] W. Steckelmacher, Vacuum 28 (1978) 269-275.

[5] M. Abramowitz, I. Stegun, Handbook of Mathematical Functions, Dover, New York, 1972.

[6] H. Risken, The Fokker-Planck Equation, Springer, 1989.

[7] G. Carrier, C. Pearson, Partial Differential Equations, Academic Press, New York, 1976.

[8] S. Chandrasekhar, Reviews of Modern Physics 15 (1943) 1.